Supporting Information

Oxidative potential of solvent-extractable organic matter of ambient total suspended particulate in Bangkok, Thailand

Jiaqi Wang [a, f], Shizhen Zhao [a,b*], Haoyu Jiang [a], Xiaofei Geng [a], Jun Li [a,b], Shuduan Mao [c], Shexia Ma [d], Surat Bualert [e], Guangcai Zhong [a,b], Gan Zhang [a,b]

[a] State Key Laboratory of Organic Geochemistry, Guangzhou Institute of Geochemistry, Chinese Academy of Sciences, Guangzhou, 510640, China

[b] CAS Center for Excellence in Deep Earth Science, Guangzhou, 510640, China

[c] Interdisciplinary Research Academy, Zhejiang Shuren University, Hangzhou 310021, China

[d] South China Institute of Environmental Sciences, Ministry of Environmental Protection, Guangzhou 510655, China

[e] Faculty of Environment, Kasetsart University, Bangkok 10900, Thailand

[f] School of Electrical Engineering, Zhengzhou University, Zhengzhou 450001, China

* Corresponding author:
Dr. Shizhen Zhao
E-mail: zhaoshizhen@gig.ac.cn

List of the Supporting Information:

Text S1. Positive matrix factorization (PMF) modeling

Fig S1. Back trajectories in (A) Dry I season (January to March 2016), (B) Wet season (April to October 2016), (C) Dry II season (November 2016 to January 2017)

Table S1. Method detection limits of PAHs, n-alkanes, hopanes, steranes, anhydrosugars, terephthalic acid, OC and EC

Table S2. Details of sampling information

Table S3. Comparison of PM concentration and OP_v measured in this study with those documented in literature

Text S1. Positive matrix factorization (PMF) modeling

Detailed concepts and applications of PMF model source apportionment can be referred in the EPA PMF 5.0 Fundamentals and User Guide (https://www.epa.gov/air-research/positive-matrix-factorization-model-environmental-data-analyses). Two input files are needed by PMF, including the sample species concentration values and equation-based uncertainties (Unc) (Xu et al., 2019). On the whole, thirteen chemical species were selected for use in PMF, which was included OP, EC, H+S, galactosan, mannosan, levoglucosan, terephthalic acid, HFAs, LFAs, n-alkanes, $\sum_{3\text{-ring}}$ PAHs, $\sum_{4\text{-ring}}$ PAHs, and $\sum_{5\text{–}6\text{-ring}}$ PAHs. As for the species uncertainties, if the concentration was less than or equal to the species-specific method detection limit (MDL), the Unc was calculated using the following equation:

$$\text{Unc}=5/6 \times \text{MDL}$$

If the concentration was greater than the MDL provided, the calculation was defined with the equation (Reff et al., 2007):

$$\text{Unc}=\text{Concentration} \times \text{Error fraction} + 1/3 \times \text{MDL}$$

The error fraction was set as 0.2 for EC, 0.2 for polar molecular markers, and 0.3 for non-polar molecular markers (Wang et al., 2019). OP was chosen as the "total variable," and missing values in the data were replaced by the species median. Three to six factors were tested and the optimal solution was determined by evaluating the change in Q/Q_{exp} in PMF (Wang et al., 2017). Q/Q_{exp} changed by 14.3% from the three to four factor model, less significant than 16.8% observed when the number of factors varied from four to five, indicating the factor number reaching five was needed to explaining the input data.

Uncertainty of PMF model is usually estimated by boot-strapping (BS), displacement (DISP), and bootstrapping with displacement (BS-DISP)(Zong et al., 2018). With three factors (fossil fuel combustion, biomass burning + higher plant emissions, plastic waste burning) were mapped above 80% of BS, while oil fume emissions were mapped 77%. At five factors, results were more stable with all factors mapped in BS above 80% (i.e., biomass burning (83%), fossil fuel combustion (100%), plastic waste burning (100%), oil fume emissions (86%), higher plant emissions (80%)), no swaps occurred with DISP and all BS-DISP runs were successfully. However, the solution became less stable in moving from five to six factors. In the six-factor solution, n-alkanes was separated from oil fume emissions and resolved into a single source without other chemical species' support. Besides the new n-alkanes factor was only mapped 59%, other factors were mapped above 90%. Thus, the five factors were chosen to be the optimal PMF solution to interpret the source profiles.

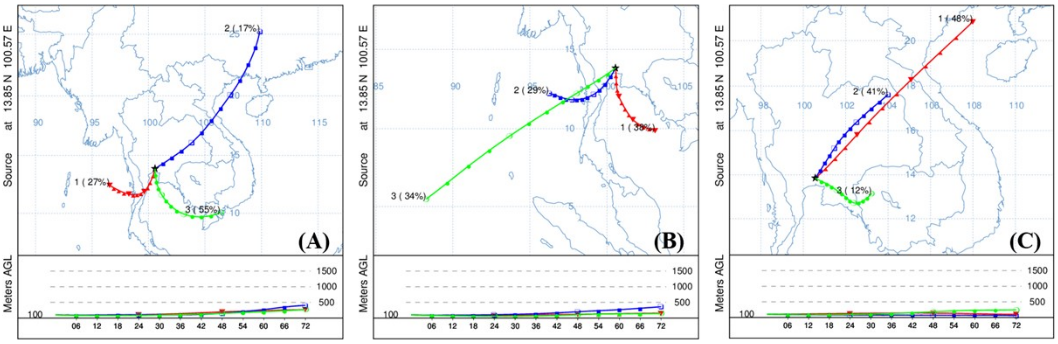

Fig S1. Back trajectories in (A) Dry I season (January to March 2016), (B) Wet season (April to October 2016), (C) Dry II season (November 2016 to January 2017).

Table S1. Method detection limits of PAHs, n-alkanes, hopanes, steranes, anhydrosugars, terephthalic acid, OC and EC.

Compounds	Method detection limit (MDL)	Compounds	Method detection limit (MDL)
PAHs (ng m^{-3})		**Hopanes and Steranes (pg m^{-3})**	
Ace	0.0017	17α(H),21β(H)-30-norhopane	10.3
Acy	0.0052	17α(H),21β(H)-hopane	78.0
Flu	0.0059	17α(H),21β(H)-22S-homohopane	19.9
Phe	0.0194	17α(H),21β(H)-22R-homohopane	8.8
Ant	0.0012	17α(H)-22,29,30-trisnorhopane	10.5
Fla	0.0045	αββ 20R-cholestane	79.5
Pyr	0.0071	ααα 20R-cholestane	12.2
BaA	0.0076	αββ 20R 24S-methylcholestane	5.92
Chr	0.0036	αββ 20R 24R-ethylcholestane	2.84
BbF	0.0021	ααα 20R 24R-ethylcholestane	10.8
BkF	0.0011	**Fatty acids (ng m^{-3})**	
BaP	0.0009	$C_{10:0}$	0.12
IcdP	0.0021	$C_{11:0}$	0.03
DahA	0.0016	$C_{12:0}$	0.18
BghiP	0.0020	$C_{13:0}$	0.11
n-Alkanes (ng m^{-3})		$C_{14:0}$	0.45
C_{13}	0.16	$C_{15:0}$	0.21
C_{14}	0.32	$C_{16:0}$	10.88
C_{15}	0.32	$C_{17:0}$	0.36
C_{16}	0.24	$C_{18:0}$	4.44

C_{17}	0.12	$C_{20:0}$	0.51
C_{18}	0.20	$C_{21:0}$	0.28
C_{19}	0.08	$C_{22:0}$	2.2
C_{20}	0.13	$C_{23:0}$	0.75
C_{21}	0.09	$C_{24:0}$	1.55
C_{22}	0.19	$C_{25:0}$	0.67
C_{23}	0.25	$C_{26:0}$	0.79
C_{24}	0.33	$C_{27:0}$	0.49
C_{25}	0.36	$C_{28:0}$	1.93
C_{26}	0.37	$C_{29:0}$	0.39
C_{27}	0.36	$C_{30:0}$	1.37
C_{28}	0.36	**terephthalic acid (ng m^{-3})**	1.17
C_{29}	0.35	**Anhydrosugars (ng m^{-3})**	
C_{30}	0.30	Levoglucosan	29.5
C_{31}	0.30	Mannosan	5.15
C_{32}	0.23	Galactosan	2.21
C_{33}	0.17	**OC (µg m^{-3})**	0.13
C_{34}	0.16		0.025
C_{35}	0.12	**EC (µg m^{-3})**	
C_{36}	0.09		

Table S2. Details of sampling information

Sample No.	Sampling date		Sampling volume (m^3)	Sample No.	Sampling date		Sampling volume (m^3)
	Start	End			Start	End	
1	2016/1/18	2016/1/19	432	45	2016/5/23	2016/5/24	432
2	2016/1/25	2016/1/26	432	46	2016/5/25	2016/5/26	432
3	2016/2/1	2016/2/2	432	47	2016/5/27	2016/5/28	432
4	2016/2/2	2016/2/3	432	48	2016/5/29	2016/5/30	432
5	2016/2/15	2016/2/16	432	49	2016/5/31	2016/6/1	432
6	2016/2/22	2016/2/23	432	50	2016/6/2	2016/6/3	432
7	2016/2/29	2016/3/1	432	51	2016/6/14	2016/6/15	432
8	2016/3/4	2016/3/5	432	52	2016/10/22	2016/10/23	432
9	2016/3/8	2016/3/9	432	53	2016/10/24	2016/10/25	432
10	2016/3/10	2016/3/11	432	54	2016/10/26	2016/10/27	432
11	2016/3/12	2016/3/13	432	55	2016/10/28	2016/10/29	432
12	2016/3/14	2016/3/15	432	56	2016/10/30	2016/10/31	432
13	2016/3/16	2016/3/17	432	57	2016/11/1	2016/11/2	432
14	2016/3/18	2016/3/19	432	58	2016/11/3	2016/11/4	432
15	2016/3/20	2016/3/21	432	59	2016/11/5	2016/11/6	432
16	2016/3/22	2016/3/23	432	60	2016/11/7	2016/11/8	432
17	2016/3/24	2016/3/25	432	61	2016/11/9	2016/11/10	432
18	2016/3/26	2016/3/27	432	62	2016/11/11	2016/11/12	432
19	2016/3/28	2016/3/29	432	63	2016/11/13	2016/11/14	432
20	2016/3/30	2016/3/31	432	64	2016/11/15	2016/11/16	432
21	2016/4/1	2016/4/2	432	65	2016/11/17	2016/11/18	432
22	2016/4/3	2016/4/4	432	66	2016/11/19	2016/11/20	432
23	2016/4/5	2016/4/6	432	67	2016/11/21	2016/11/22	432
24	2016/4/7	2016/4/8	432	68	2016/11/23	2016/11/24	432
25	2016/4/9	2016/4/10	432	69	2016/11/25	2016/11/26	432
26	2016/4/13	2016/4/14	432	70	2016/11/27	2016/11/28	432
27	2016/4/15	2016/4/16	432	71	2016/11/29	2016/11/30	432
28	2016/4/17	2016/4/18	432	72	2016/12/1	2016/12/2	432
29	2016/4/19	2016/4/20	432	73	2016/12/3	2016/12/4	432
30	2016/4/21	2016/4/22	432	74	2016/12/5	2016/12/6	432
31	2016/4/23	2016/4/24	432	75	2016/12/7	2016/12/8	432
32	2016/4/25	2016/4/26	432	76	2016/12/9	2016/12/10	432
33	2016/4/27	2016/4/28	432	77	2016/12/11	2016/12/12	432
34	2016/4/29	2016/4/30	432	78	2016/12/13	2016/12/14	432
35	2016/5/1	2016/5/2	432	79	2016/12/15	2016/12/16	432
36	2016/5/3	2016/5/4	432	80	2016/12/17	2016/12/18	432
37	2016/5/5	2016/5/6	432	81	2016/12/20	2016/12/21	432
38	2016/5/9	2016/5/10	432	82	2016/12/27	2016/12/28	432
39	2016/5/11	2016/5/12	432	83	2017/1/3	2017/1/4	432

40	2016/5/13	2016/5/14	432	84	2017/1/7	2017/1/8	432
41	2016/5/15	2016/5/16	432	85	2017/1/14	2017/1/15	432
42	2016/5/17	2016/5/18	432	86	2017/1/21	2017/1/22	432
43	2016/5/19	2016/5/20	432	87	2017/1/28	2017/1/29	432
44	2016/5/21	2016/5/22	432				

Table S3. Comparison of PM size, concentration and OP_v measured in this study with those documented in literature

	Bangkok[a]	Netherland[b]	Guru Shikhar[c]	Milan[d]	Lecce[e]
Size	TSP	PM_{10}	PM_{10}	TSP	PM_{10}
PM, $\mu g\ m^{-3}$	56.3 ± 32.1	41.2	96 ± 56 (29-273)	50 ± 7	33 ± 13
OP_v, nmol DTT $min^{-1} m^{-3}$	1.5 ± 0.5	3.54 (2.19-6.65)	1.23 ± 0.68 (0.09-3.04)	0.1 ± 0.05	0.21 ± 0.12 (0.02-0.53)

[a] (Present study, Bangkok)

[b] (Janssen et al., 2014)

[c] (Patel and Rastogi, 2018)

[d] (Perrone et al., 2016)

[e] (Pietrogrande et al., 2018)

References

Janssen, N.A.H., Yang, A., Strak, M., Steenhof, M., Hellack, B., Gerlofs-Nijland, M.E., Kuhlbusch, T., Kelly, F., Harrison, R., Brunekreef, B., Hoek, G., Cassee, F., 2014. Oxidative potential of particulate matter collected at sites with different source characteristics. Science of The Total Environment 472, 572-581.

Patel, A., Rastogi, N., 2018. Seasonal variability in chemical composition and oxidative potential of ambient aerosol over a high altitude site in western India. Science of The Total Environment 644, 1268-1276.

Perrone, M.G., Zhou, J., Malandrino, M., Sangiorgi, G., Rizzi, C., Ferrero, L., Dommen, J., Bolzacchini, E., 2016. PM chemical composition and oxidative potential of the soluble fraction of particles at two sites in the urban area of Milan, Northern Italy. Atmospheric Environment 128, 104-113.

Pietrogrande, M.C., Perrone, M.R., Manarini, F., Romano, S., Udisti, R., Becagli, S., 2018. PM 10 oxidative potential at a Central Mediterranean Site: Association with chemical composition and meteorological parameters. Atmospheric Environment 188, 97-111.

Reff, A., Eberly, S.I., Bhave, P.V., 2007. Receptor modeling of ambient particulate matter data using positive matrix factorization: Review of existing methods. Journal of the Air & Waste Management Association 57, 146-154.

Wang, Q.Q., He, X., Huang, X.H.H., Griffith, S.M., Feng, Y.M., Zhang, T., Zhang, Q.Y., Wu, D., Yu, J.Z., 2017. Impact of secondary organic aerosol tracers on tracer-based source apportionment of organic carbon and PM2.5: A case study in the Pearl River Delta, China. Acs Earth and Space Chemistry 1, 562-571.

Wang, Q.Q., Huang, X.H.H., Tam, F.C.V., Zhang, X.X., Liu, K.M., Yeung, C., Feng, Y.M., Cheng, Y.Y., Wong, Y.K., Ng, W.M., Wu, C., Zhang, Q.Y., Zhang, T., Lau, N.T., Yuan, Z.B., Lau, A.K.H., Yu, J.Z., 2019. Source apportionment of fine particulate matter in Macao, China with and without organic tracers: A comparative study using positive matrix factorization. Atmospheric Environment 198, 183-193.

Xu, H., Xiao, Z.M., Chen, K., Tang, M., Zheng, N.Y., Li, P., Yang, N., Yang, W., Deng, X.W., 2019. Spatial and temporal distribution, chemical characteristics, and sources of ambient particulate matter in the Beijing-Tianjin-Hebei region. Science of the Total Environment 658, 280-293.

Zong, Z., Wang, X., Tian, C., Chen, Y., Fu, S., Qu, L., Ji, L., Li, J., Zhang, G., 2018. PMF and PSCF based source apportionment of PM2.5 at a regional background site in North China. Atmospheric Research 203, 207-215.